



Mass transfer of differently sized organic solutes at spacer covered and permeable nanofiltration wall

Emil Dražević^{a,*}, Krešimir Košutić^a, Vladimir Dananić^b

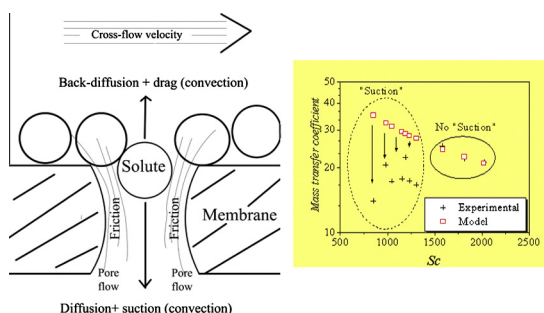
^a Department of Physical Chemistry, University of Zagreb, Faculty of Chemical Engineering and Technology, Marulićev trg 19, HR-10000 Zagreb, Croatia

^b Department of Physics, University of Zagreb, Faculty of Chemical Engineering and Technology, Marulićev trg 19, HR-10000 Zagreb, Croatia

HIGHLIGHTS

- Cross-flow velocity significantly affects removal of organics.
- Sherwood relation correctly estimates mass transfer at small solute fluxes.
- At high solute fluxes Schmidt number needs correction.
- Correction correlation is proposed for Schmidt number.

GRAPHICAL ABSTRACT



ARTICLE INFO

Article history:

Received 12 September 2013

Received in revised form 2 January 2014

Accepted 20 January 2014

Available online 31 January 2014

Keywords:

Nanofiltration

Porosity

Concentration polarization

Pore size distribution

Mass transfer coefficient

ABSTRACT

Concentration polarization (CP) phenomena may significantly affect water permeability and removal of organics solutes in cross-flow nanofiltration (NF) making it an important optimization parameter. Most of the models predict CP using mass transfer coefficients that may be estimated using model Sherwood (Sh) relations of a general form, $Sh = a^* Re^b Sc^c$. In many cases Sh relations are able to predict mass transfer coefficients remarkably well; however, such relations are in general valid only for non-permeable walls. Sh relations were experimentally validated using a binary solution of single solute and water where Schmidt numbers (Sc) were varied by changing the temperature or density of the solution, at a constant or varied Reynolds number (Re). This study evaluated Sh relations from different angle and used ten organic solutes of different diffusivity at a constant concentration and viscosity of solutions, covering a range of Sc from 850 to 2022. The aim of this study was to evaluate the Sh relation in predicting the mass transfer of differently sized organic solutes in rectangular channel, at spacer covered and permeable NF wall of defined porosity. Comparison of experimental Sh , obtained using the velocity variation method, and model Sh showed that model Sh relation correctly predicts mass transfer of organics when particular solute flux through the NF permeable wall is sufficiently low. A correction correlation is proposed for coefficient c on Sc in model Sh relation, where c approaches the model Sh value, 0.42, with the increase in size of the solutes. In addition, data presented show that the removal of organic solutes from the water may be significantly improved, up to 280%, by changing the hydrodynamics in the channel.

© 2014 Elsevier B.V. All rights reserved.

1. Introduction

Nanofiltration (NF) membranes have been widely applied to drinking water treatment [1], industrial effluent treatment [2],

water softening [3], or concentration of grass juice [4]. NF processes usually remove most of the solutes from water, thus solutes tend to accumulate on the membrane surface developing a concentration polarization (CP) layer. Given that NF processes are pressure and concentration driven processes [5], enhanced concentration at the membrane surface may significantly [6] affect the NF

* Corresponding author. Tel.: +385 14597240.

E-mail address: edraz@fkit.hr (E. Dražević).

performance in terms of flux reduction and removal of solutes [7]. In this context, CP could be considered as one of the important parameters in NF process optimization. Many studies dealt with CP phenomena [8,9] and its effect on removal of salts or mixture of salts [10], but very few of them systematically examined CP effect on removal of organics [7], particularly in nanofiltration. NF processes are also of increasing use in removal of organic solutes [1,11] and it is important to correctly evaluate the impact of hydrodynamic conditions on their removal as well as to properly address this phenomena. Most models which describe CP in cross-flow nanofiltration require a knowledge of mass transfer coefficients [12].

Mass transfer coefficients may be determined experimentally, e.g., using the velocity variation method (VVM) [13] or electrochemical methods [14]. VVM has been known for decades as a simple and efficient method applicable to solutes that are not completely rejected by the membrane [8]. VVM is, however, often criticized because the boundary layer in a RO/NF channel is undeveloped and of a non-uniform thickness. Assuming its uniformity can produce significant errors because local concentration at the membrane wall varies throughout the channel [6,15]. A feed spacer may be used as a promoter of turbulence and local mixing where each mesh on the spacer periodically interrupts the development of boundary layer; in these cases the thickness of the boundary layer could be considered uniform and static. Indeed, a recent numerical simulation of mass transfer in a spacer filled channel [14] has shown that for $Re > 159$ and $Sc > 100$, the boundary layer is becoming closer to uniformity.

Mass transfer coefficients may be determined as well using model Sh relations, which are valid for channels with non-permeable walls [8,16]. NF membranes are economically viable because they offer high water fluxes. At higher water fluxes, however, a significant “suction” occurs and NF membranes cannot be considered as non-permeable walls. “Suction” may significantly affect the mass transfer coefficient and thus enhance concentration polarization [17] where membrane porosity and pore sizes may play a substantial role. Previous studies showed that membranes, which can be considered as permeable walls at significantly high fluxes, may vary in terms of thickness and swelling [18] as well as heterogeneity [19]. Košutić et al. reported that reverse osmosis membranes have denser and less porous structures compared to NF membranes [20]. Both pore size distributions and number of pores (active porosity) of membranes cannot be simply evaluated since the radii of the pores of NF membranes are below 1 nm [21]. Therefore, an indirect method was used in this paper, similar as reported earlier [22], to evaluate pore size distribution and the number of pores, i.e., active porosity of the membrane representing the permeable wall.

In this context, this study aims at checking the validity of model Sh relation in predicting the mass transfer coefficients in rectangular channels with one highly permeable and porous wall. Experimental average mass transfer coefficients of organic solutes, which differ in molecular mass and diffusivity, were estimated using VVM and afterwards compared with model Sh relations, which well described hydrodynamic conditions in this work [14]. The organic solutes were chosen to cover a range of Sc which are of particular interest for NF, ranging from 850 to 2022. Highly permeable wall considered herein was commercial high flux NF membrane, NF270, while mass transfer coefficients were studied at a permeation velocity of $40 \mu\text{m s}^{-1}$, when significant “suction” occurs [23].

2. Theoretical background

2.1. Sherwood relation

The Sh relation that fully describes hydrodynamic conditions in the system [24] is described using general expression below.

$$Sh = \frac{kd_H}{D} = aRe^bSc^c \left(\frac{d_H}{L}\right)^d \quad (1)$$

Eq. (1) is used to estimate mass transfer coefficients while the empirical coefficients a , b , c and d may be found in literature and depend on hydrodynamic conditions and feed spacer characteristics [8,14,16]. The Re in Eq. (1) is calculated as $Re = (u d_H)/\nu$, and Sc as $Sc = \nu/D$, where u is cross-flow velocity in the channel, d_H hydraulic diameter, D is diffusivity, and ν is kinematic viscosity. The height and the length of the channel are constant and Eq. (1) may be simplified taking $a^* = a (d_H/L)^d$:

$$Sh = a^* Re^b Sc^c \quad (2)$$

Hydraulic diameter, d_H , for a rectangular channel with the spacer in the channel was calculated as proposed by Shock and Miquel [25].

$$d_H = \frac{4P}{2/h + (1-P)(S_{SP}/V_{SP})} \quad (3)$$

In Eq. (3) P is the porosity of the spacer, $P = 1 - V_{SP}/V_{TOT(SP)}$, S_{SP} is the surface of the spacer, V_{SP} is the volume of the spacer, and $V_{TOT(SP)}$ total volume of the spacer. Average velocity of fluid can be calculated as proposed below.

$$u[\text{m s}^{-1}] = \frac{Q[\text{m}^3 \text{s}^{-1}]}{P_{FC}A[\text{m}^2]} \quad (4)$$

where Q is feed flow rate and A is cross-sectional area of the channel and P_{FC} porosity of the channel expressed as $P_{FC} = V_{SP}/V_{FC}$, where V_{FC} is the volume of the channel.

2.2. Mass transfer coefficients – VVM and model Sh relation

VVM [13] is used in this study to assess experimental mass transfer coefficients.

$$\ln\left(\frac{1-f}{f}\right) = \ln\left(\frac{1-f_m}{f_m}\right) + \frac{J_v}{k} \quad (5)$$

In Eq. (5), mass transfer coefficient, k , can be approximated [6] as $k \approx K \cdot u^B$ where u is average cross-flow fluid velocity. Eq. (5) is used in a simple experimental procedure where u is varied at constant J_v and constant temperature while rejection, f , and cross-flow velocity, u , are measured. A fit to the experimental data gives the constant K which is used to approximate average mass transfer coefficient in the channel as well as the true membrane rejection, f_m . The value of coefficient B has to be set before fitting and this study takes B as proposed below. By combining Eqs. (1) and (2), the mass transfer coefficient of one solute can be calculated as presented below.

$$k = a^* \frac{D}{d_H} Re^b Sc^c \quad (6)$$

In Eq. (6), Re is the only variable while other parameters are constant because only one solute is considered in a diluted feed solution at a constant temperature and in constant geometry of the channel. Eq. (6) can be rewritten as proposed below, where terms in elongated brackets represent the constant.

$$k = \left\{ a^* \frac{D}{d_H} Sc^c \left(\frac{d_H}{\nu}\right)^b \right\} u^b \quad (7)$$

The analogy may be noticed between $k = K u^B$ in Eqs. (5) and (7). Parameter B in Eq. (5) can be taken as coefficient b on Re number in Sh relation, which is usually available in literature. The parameters b , c and B , which correspond to geometry of the feed spacer used ($l_M/d_f = 12$ and $\beta = 90^\circ$), and hydrodynamic conditions in the channel are taken from the work of Koutsou et al. [14]. Theoretical mass transfer coefficient, k , in our system can then be calculated as presented below.

$$k = 0.126Re^{0.57}Sc^{0.42} \frac{D}{d_H} \quad (8)$$

When a suitable correlation for mass transfer coefficient exists, such as Eq. (8), then a “suction” mass transfer correction factor [17] may be used to estimate the mass transfer coefficient, k_s , at higher permeation velocities, i.e., “suction.”

$$k_s = \left[\frac{J_v}{k} + \left(1 + 0.26 \left(\frac{J_v}{k} \right)^{1.4} \right)^{-1.7} \right] k \quad (9)$$

2.3. Pore size distribution, number of pores and active porosity of NF270 membrane

Pore size distribution (PSD) was calculated using the Surface Force – Pore Flow (“SF-PF”) model which was developed and thoroughly described by Sourirajan and Matsuura [26]. Briefly, fundamentals of this model are as follows: the pores in the skin layer are assumed to be cylindrical and solute to membrane interactions relative to water can be described as Lennard–Jones surface potential functions. A thorough description of the calculation procedure used in this study is found in a recent study of Dražević et al. [22]. Rejections, f , and permeation velocities, J_v , of six different solutes, trimethylene oxide, 1,3-dioxolane, 1,4-dioxane, 12-crown-4, 15-crown-5 and 18-crown-6, have been experimentally obtained. The calculation procedure employed herein is searching the pore size distribution and the number of pores by minimizing the deviations between experimental and theoretical rejections and permeation velocities of all six solutes. Once average pore radii and their numbers for a particular membrane are calculated, active porosity of RO/NF membrane can be estimated using Eq. (10), where i is the number of dominant peaks in PSD, r_i is the dominant pore radius, N_i is the number of pores of r_i average radii, and A is the working surface of the membrane in the SEPA II cell, 0.0138 m². Dominant pore radius with the highest number of pores was taken as the average pore radius.

$$\varepsilon = \sum_{i=1}^n \pi r_i^2 N_i / A \quad (10)$$

3. Experimental

3.1. Membranes and materials

The commercial nanofiltration membrane NF270 (Dow/Filmtec, Midland, MI, USA) has been used in this study. Organic solutes used are summarized in Table 1.

Diffusion coefficients in Table 1 were estimated using Wilke–Chang relation [27,28]:

$$D_{AW} = 7.4 \cdot 10^{-8} \frac{(\Psi \cdot M_W)^{0.5} \cdot T}{\eta_W \cdot V_A^{0.6}} \quad (11)$$

Table 1

Characteristics of organic solutes (purity, origin, molar mass, diffusion coefficients in water, Sc numbers and corresponding Stokes radii).

Organic solute	Manufacturer	M (g mol ⁻¹)	D (10 ⁻¹⁰ m ² s ⁻¹)	Sc, $T = 298$ K	r_{St} (nm)
Trimethylene oxide, 97%	Acros Organics, New Jersey, USA	58.08	11.8	850	0.185
1,3-Dioxolane, 99.8%	Sigma–Aldrich, USA	74.08	11.0	912	0.198
Glycerol, 98%	Veblaborchemie, Apolda, Germany	92.09	10.2	983	0.214
1,4-Dioxane, 99.8%	Sigma–Aldrich, USA	88.11	9.6	1046	0.227
Erythritol, min 99%	Sigma–Aldrich, USA	122.12	8.7	1153	0.251
1,4-Cyclohexanedione, 99%	Fluka, Switzerland	112.13	8.4	1192	0.259
Cyclohexanol, 98 %	Riedel-De Haen Ag Seelze, Germany	100.16	8.1	1232	0.268
Pinacol, 99%	Sigma–Aldrich, USA	118.17	7.7	1308	0.284
12-Crown-4, purum; ≥98%	Fluka, Switzerland	176.21	6.3	1585	0.345
15-Crown-5, >98%	Merck-Schuchardt, München, Germany	220.27	5.5	1814	0.395
18-Crown-6, ≥99.5% (GC)	Fluka, Switzerland	264.32	4.9	2022	0.440

where η is viscosity of water (Pa s), T temperature (K), $\Psi = 2.26$, factor considering water, M_W molar mass of water (kg mol⁻¹), a V_A Le Bass molar volume of solute A (m³ mol⁻¹).

3.2. NF setup and experimental conditions

The NF/RO apparatus used in this study is schematically shown in Fig. 1. NF experiments were carried out in a cross flow Sepa CF II cell (Sterlitech Corporation, USA) of a membrane area 0.0138 m² and channel dimensions 14.5 × 9.5 × 0.02 cm³ (length × width × height). Inside angles of the spacer’s mesh were 90° while the angle towards the flow was 90°. The dimensions of the mesh of the spacers (14.5 × 9.5 cm²) were as follows, thickness of the filament, $d_f = 0.4$ mm, length of the mesh, $l_M = 4.6$ mm and the thickness of the spacer, $h_{SP} = 1.2$ mm, therefore the corresponding porosity of the spacer was, $P = 0.377$ and porosity of the channel, $P_{FC} = 0.83$.

The feed from a 5 L tank was circulated through the cell at different flow rates (1–5 L min⁻¹) by means of a Hydracell DO3SAS-GSSSCA pump driven by a variable speed motor (Wanner engineering inc., Minneapolis, USA). The volume flux through the membrane, J_v , was determined by collecting and weighing the permeate over a certain time at constant temperature (25.0 ± 0.1 °C). The temperature was held constant by the use of a water bath and Danfoss XG10 heat exchanger. Experiments with a NF270 membrane were performed at 1.10 MPa (11.0 bar).

Feed solution concentration of each organic solute was 0.1 g L⁻¹ (100 ppm). Prior to each measurement the flux was stabilized at 2.2 MPa (22.0 bar) for 2 h, and experiments thereafter were carried out in recycle mode for each organic solute by changing the flow-rate in the order from highest to lowest and then repeated in reverse order. Concentration of organic solutes in feed and permeate was determined using a Total Organic Carbon Analyser (Shimadzu TOC V_{WS}).

4. Results and discussions

4.1. NF270 properties – pore size distribution and active porosity

Pore sizes and number of pores have been estimated using data on the thickness of swelled NF270 selective layer, 19 nm [18], and data on measured rejection of six disc like molecules and permeation velocities using calculation procedure described recently by Dražević et al. [22]. Pore sizes and their corresponding numbers, which are summarized in Table 2, are fairly similar to recent estimates of NF270 membrane [22]. Semiao et al. [29] have recently got an identical average pore radius for the NF270 membrane, 0.40 nm, while bigger pores (defects) are reported in a TEM study on the NF270 membrane [30].

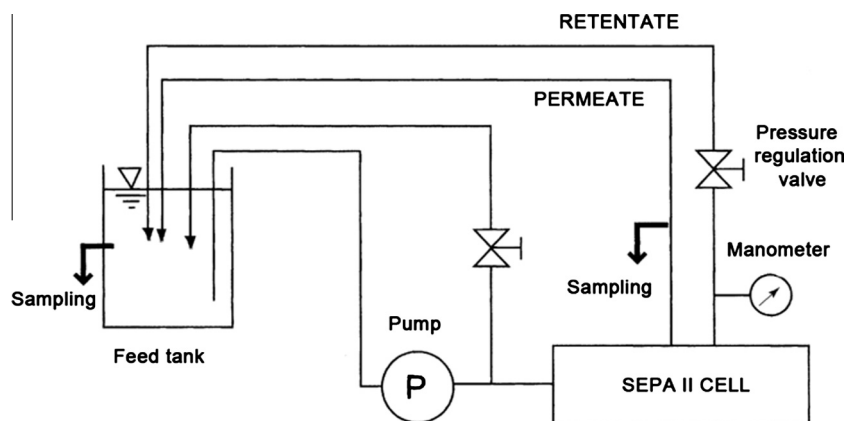


Fig. 1. SEPA II membrane unit.

Table 2

NF270 structural properties. Data on pore radii, number of pores and porosity were obtained using described calculation procedure and Eq. (10), while the AFM data taken from Freger [18].

AFM data		Dominant radii		Number of pores		Porosity	
ΔX_{dry}	ΔX_{wet}	r_1 (nm)	r_2 (nm)	N_1	N_2	ε	$L_p \text{ Lm}^{-2} \text{ h}^{-1} \text{ bar}^{-1}$
14.1	19	0.40	1.00	1.19E+15	1.09E+13	0.048	12.5

Assuming, however, the real pores (voids) in the NF270 selective layer are cylindrical, hydrodynamic resistance is directly correlated with the thickness of the selective layer, ΔX_{wet} , which significantly affects calculated surface porosity. Hydrodynamic resistance is also minimized due the fact velocity inside the pore is considered constant in time and not rotational. These simplifications in the model made the thickness parameter, ΔX_{wet} , as the dominant parameter in setting the scale of the total number of pores, i.e., porosity, Eq. (10). Because of this simplification, the real porosity of the membrane should be even greater than the calculated porosity (4.8%) simply because the hydrodynamic resistance of the real and tortuous pore, of the same thickness, is greater than the one of idealized and straight cylindrical pore. In this sense, the “real” porosity of this membrane should be several times higher, which is indicated by the measured high water volume fraction, 20% [18]. It then appears that NF270 shows high water permeability (L_p , Table 2) because of its very thin selective layer, 19 nm [18], and relatively high porosity. For this reasons NF270 could be very suitable for VVM because solute transport across the NF270 layer could be very sensitive to any change in concentration near the membrane surface [22]. In addition, higher porosity of NF270 may add to a more regular buildup of a polarization layer on the membrane surface.

4.2. Cross-flow velocity effect on measured rejection, f , of organic solutes- correlation to Stokes radii of organic solutes

Fig. 2A plots the measured rejection of three representative organic solutes, differing in size, at different cross-flow velocities. It should be noted that data reported herein are probably valid only for the rectangular cell used in this study and may not entirely hold in some other geometry, for instance tubular module where CP is less pronounced. Nevertheless, data presented indicate that the measured rejection strongly depends on hydrodynamic conditions making CP an important parameter in optimizing the NF performance for the best removal of a particular organic solute. Fig. 2B shows relative changes in rejection from a remarkable 280% for smallest solute, to only 6% for biggest solute.

A change in measured rejection obtained with an increase in cross-flow velocity might be related to structural properties of the NF270 selective layer, such higher porosity and its being extremely thin. Both of these properties could make NF270 sensitive to changes in concentrations at the membrane surface. For instance, concentration of the solute at the membrane surface is directly related to mass transfer coefficient in the channel [12]. At a constant permeation velocity logarithm of mass transfer coefficient is proportional to average cross-flow fluid velocity, Eq. (7), and its increase is directly reducing the concentration of the solutes at the membrane surface. Since concentration of a solute at the membrane surface is directly affecting the solute flux across NF270 selective layer, solute flux becomes lower which results with an increase in measured rejection. A recent study on NF270 reported similarly high changes in rejections of organic solutes, which were attempted to correlate to the change in concentration of solutes near the membrane wall [22]. It should be noted though, in the aforementioned study [22] the concentrations of solutes near the membrane wall were manipulated quite differently. Membrane was modified with hydrophilic layer, i.e. the affinity of membrane was changed which dramatically affected the rejections of organic solutes, measured at a constant cross-flow velocity.

Brian [12] suggested a concentration of a solute at the membrane wall in cross-flow conditions depended highly on the membrane rejection of the particular solute, permeation velocity, and mass transfer coefficient. According to Brian, at a constant permeation velocity, concentrations of poorly rejected solutes (Fig. 2A) should be just slightly above the corresponding concentrations in the bulk solution. The smallest and poorly rejected solutes, however, show the highest measured changes in rejection while the biggest solutes show very small change in rejection with cross-flow velocity. For instance, trimethylene oxide rejection increased from 9% to 24% while that of biggest 18-crown-6 changed from 87% to 95%. Note that the rejection of organic solutes depends on the solute size and the average pore size [31]. The bigger is the solute, the higher is the friction between the pore wall and the solute and the lower is the solute flux (Fig. 3). The higher the friction, the membrane is less sensitive to the changes in the concentrations

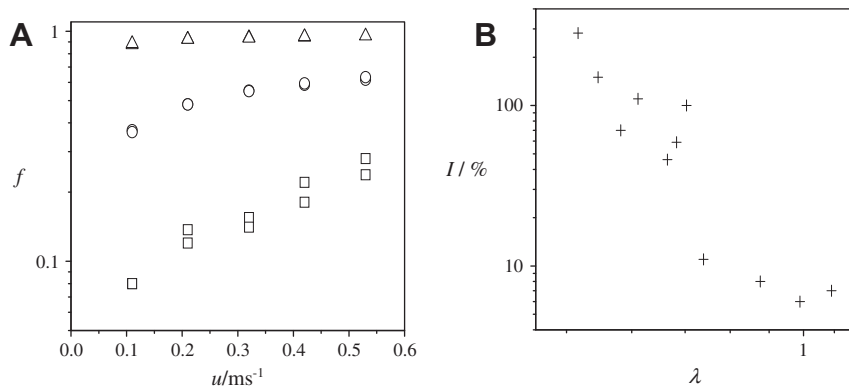


Fig. 2. The effect of cross-flow velocity on measured rejection: (A) trimethylene oxide (□), glycerol (○) and 18-crown-6 (Δ); (B) the relative difference in rejection, $I/\% = \{[f(u = 0.56) - f(u = 0.11)]/f(u = 0.11)\} \cdot 100$, versus $\lambda = r_{\text{sol}}/r_{\text{p}}$ (NF270), $r_{\text{p}} = 0.40$ nm.

at the membrane surface. Obviously, friction force between small organic solutes, such as trimethylene oxide, and pore wall is small thus making NF270 membrane sensitive to change in concentration of small solutes (driving force) at its surface. The rejection of trimethylene oxide, however, could not be expected to increase much more above 30% since at highest cross-flow velocity used its concentration near the membrane surface was probably close to that of a bulk.

In order to facilitate the discussion let us consider the solute at the entrance of the pore and the forces acting on it, which is well illustrated in Fig. 3. At a constant permeation velocity, the “suction force” that pulls the particular solute into the membrane pore may be considered constant and in major part balanced by the friction force and back-diffusion solute drag. Note that back-diffusion drag is proportional to the mass transfer coefficient and the difference in concentrations at the membrane surface and in the bulk. One may conclude from Fig. 2 that back-diffusion drag weakly affected the overall measured rejection because the change in cross-flow velocity poorly affected the rejection of bigger solutes. It is apparent then that the “suction” force is in major part balanced only by the friction force which depends on the solute and the pore size. It is then suggested that change in rejection of smaller solutes should be related to solute size and structural properties of the NF270, more precisely to the solute/average pore radii ratio, λ (Fig. 2B).

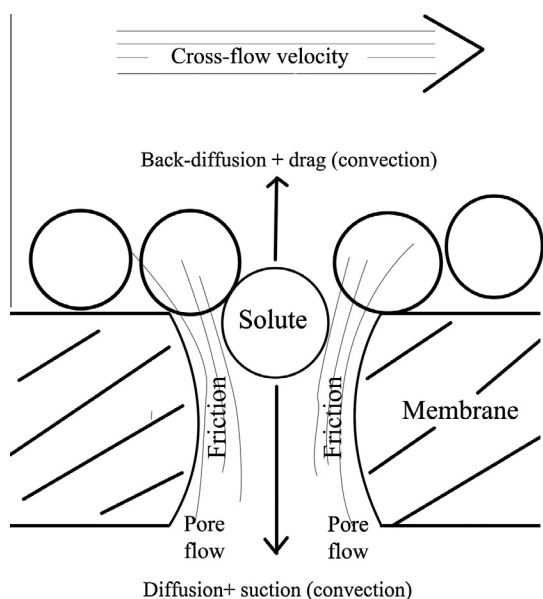


Fig. 3. Forces acting on a solute at the entrance of the pore.

Parameter λ is widely applied in hindrance factor relations [32] for predictive purposes of hindered transport of solutes in water-filled pores. In this sense, λ may be used as a parameter correlating to the solute/membrane friction force (Fig. 3). Data presented in Fig. 2B show a strong correlation of the relative change in measured rejection and solute/pore radii ratio, λ . It can be re-confirmed, referring to Fig. 2B, that at higher and constant permeation velocity, analogous to the one used in this study, a significant “suction” of smaller solutes [17] occurred. The effect of “suction” on the back-diffusion drag, i.e. mass transfer coefficients, is discussed in the following sections.

4.3. Comparison of model and experimental values of mass transfer coefficient – correlation to solute flux

Mass transfer coefficients are experimentally obtained using Eq. (5) as showed in Fig. 4. Values of K are estimated by linear regression and used to calculate average mass transfer coefficients in analogy with Eq. (7), i.e., $k_{\text{exp}} = K u^{0.57}$, where K is approximated from two independent measurements (Fig. 4). Table 3 summarizes the measured mass transfer coefficients with corresponding constant K paired with coefficient of determination, R^2 . Assumption on uniform film thickness in spacer filled channels could be considered fairly valid, given that the average errors, measured through coefficient of determination, are fairly small (Table 3).

Fig. 5A compares experimentally obtained mass transfer coefficients (Table 3), with model k , which are obtained using Eq. (8) [14]. Curiously experimental and model values of k show two opposite trends for small Sc numbers where both become consistent at higher Sc numbers, when the rejection of the solutes is sufficiently high, $f > 85\%$.

Let us consider “suction” as solute flux through the membrane pore. Solute fluxes, J_s , which are summarized for the examined solutes in Fig. 5B, may be calculated using experimentally obtained concentration and permeation velocities, as $J_s = J_v C_p$, where C_p , mol m^{-3} , is the solute concentration in the permeate. Data showed in Fig. 5B suggest that the mass transfer coefficients of small organic solutes are much smaller than ones predicted by the Sh relation because solute flux of smaller solutes (Fig. 5B) is up to thirty times higher compared to the bigger solutes, i.e. there is a strong drag of smaller solutes into the NF270 pores. Solute flux of lower Sc numbers have higher diffusivities (smaller Stokes radius) in water and, in general, lower molecular mass which makes them more susceptible to “suction”.

Curiously, the mass transfer coefficient of 1,4-cyclohexanedione (CHD), whose rejection by NF270 is about 50%, is overestimated in lesser proportion compared to other solutes within the similar

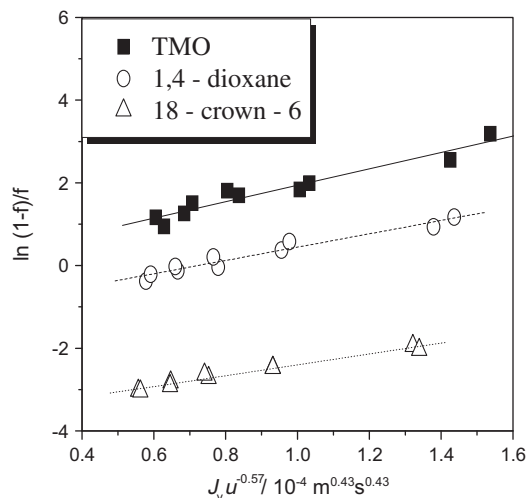


Fig. 4. Representative examples of velocity variation method used to estimate mass transfer coefficients of three different solutes on NF270. Lines represent fits obtained by linear regression, at $J_v \approx 40 \mu\text{m s}^{-1}$.

Table 3

Values of constant K and mass transfer coefficient, k_{exp} at $u = 0.11 \text{ ms}^{-1}$. Data presented are obtained from linear regression of experimental data on NF270 membrane, $J_v \approx 40 \mu\text{m s}^{-1}$.

Organic solute	$K/10^{-5}$	R^2	$k_{\text{exp}} (\mu\text{m s}^{-1})$
Trimethylene oxide	4.93	0.935	14.0
1,3-Dioxolane	4.61	0.953	13.1
Glycerol	7.25	0.983	20.6
1,4-Dioxane	6.09	0.953	17.3
Erythritol	6.26	0.978	17.8
1,4-Cyclohexanedione	7.88	0.961	22.4
Cyclohexanol	6.12	0.990	17.4
Pinacol	5.84	0.959	16.6
12-Crown-4	8.87	0.959	25.2
15-Crown-5	7.74	0.936	22.0
18-Crown-6	7.46	0.977	21.2

range of Sc . In addition, solute flux of CHD is similar to solute flux of the other solutes of similar Sc numbers, of about $25 \mu\text{mol m}^{-2} \text{ s}^{-1}$. The difference between the theoretical and experimental mass transfer coefficient of CHD, however, is about 20%, as shown in Fig. 5A. This implies that the solute flux is not the only parameter that sets the scale of k and that solute/membrane energy of interaction may play a substantial role, as reported earlier for rejection of solutes [22,33–35]. In this context, repulsion between the CHD and the membrane surface could explain the smaller difference

between theoretical and experimental k , although, such statements should be verified by additional work which exceed the topic of the present study. Nevertheless, it is apparent that the solute flux is the dominant parameter.

Bigger crown ethers (12-crown4, 15-crown-5 and 18-crown-6) showed relatively good congruence of experimental and model data on mass transfer coefficients (circled area in Fig. 5A) suggesting that at solute fluxes equal or below $2.5 \mu\text{mol m}^{-2} \text{ s}^{-1}$ (Fig. 5B) one may expect fairly good estimates of mass transfer coefficients using Sh relation. It should be mentioned as well that good congruence of experimental and model data on k of crown ethers is also direct proof of choosing the right coefficient B in Eq. (5) using the analogy with Eq. (7).

Theoretical k may be corrected for “suction” with a correction factor proposed by Geraldés and Afonso [17], using Eq. (9), which is developed using computer flow dynamics for an idealistic case when the membrane rejection is 100%. Geraldés and Afonso claim that the proposed correction factor for k is valid within the ranges of $0.10 < f \leq 0.999$, and $J_v/k < 20$. Such “suction” corrected mass transfer coefficients are presented in Fig. 5A along with our experimental and model k . It may be noted that “suction” corrected mass transfer coefficients clearly differ from both experimental and model k indicating such correction is not valid for system involved. Such correction clearly overestimates the mass transfer coefficient, probably because it assumed 100% rejection of solutes, which is unrealistic. In other words, Geraldés and Afonso assumed no solute flux through the membrane. For this reason, their modelling probably predicts an increase in concentration of solutes at the membrane surface which consequently increase only the back-diffusion of solutes from the membrane surface to the bulk solution, however, not the diffusion of solutes through the membrane at the permeate side.

4.4. Numerical evaluation of Sh versus Re relations – correction factor for coefficient c on Sc

The experimental and theoretical Sh are compared in Fig. 6. Experimental Sh was calculated using Eq. (1) and known values of k_{exp} , D and d_H . The theoretical Sh relation [14] (Fig. 6A) absolutely overestimates the Sh number for lower Sc number, when coefficient on Sc is taken as $c = 0.42$ [14]. Clearly, such an overestimate is attributed to high solute fluxes of smaller organic solutes. For this reason experimental data on Sh and Re were fitted to the model $Sh = 0.126 Re^{0.57} Sc^c$, where c was taken as the fitting parameter (Fig. 6A and B). It may be noticed the fitted model described the experimental data on Sh versus Re remarkably well and that the coefficient c appeared to be different for each solute tested (Fig. 7). Coefficient c was found to strongly correlate with solute/pore size radii ratio, λ , i.e., friction between pore wall and the

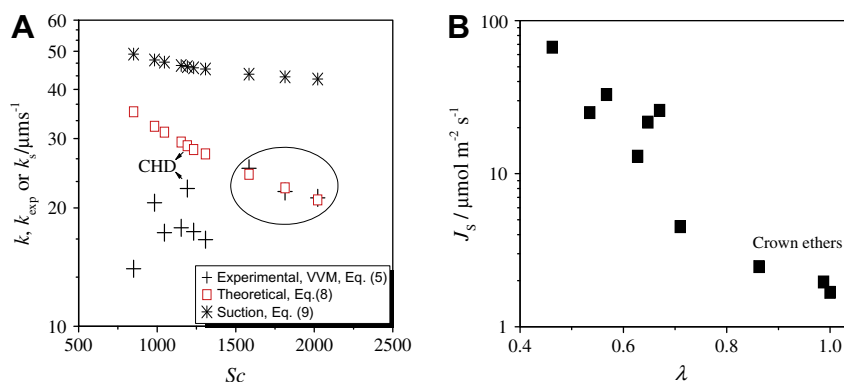


Fig. 5. Evaluation of experimental and theoretical mass transfer coefficients: (A) comparison of experimental, k_{exp} , and theoretical k and k_s , versus Sc number, $Re = 118$; (B) solute flux, $J_s = J_v C_p$, versus solute radius/average pore radius ratio, λ , at $Re = 118$.

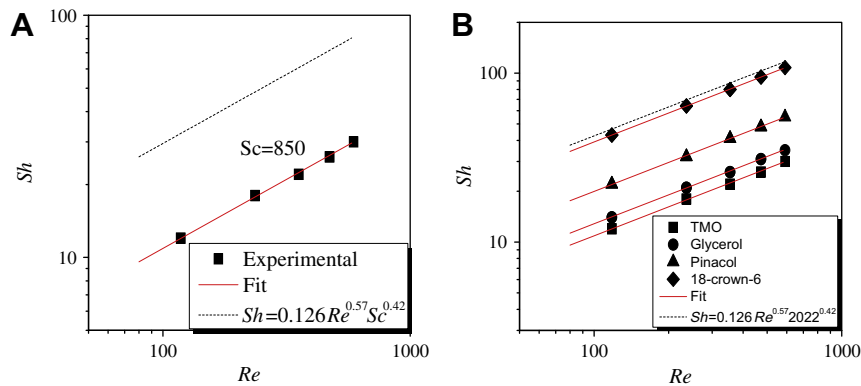


Fig. 6. Comparison of the experimental and theoretical data on Sh ; data presented are the average of two independent measurements: (A) trimethylene oxide (TMO), $Sc = 850$, experimental and model estimated Sh number [14]. A fit was obtained by varying the coefficient c in $Sh = 0.126 Re^{0.57} Sc^c$; (B) comparison of experimental, theoretical and fitted Sh at $Sc = 2022$ and some other Sc .

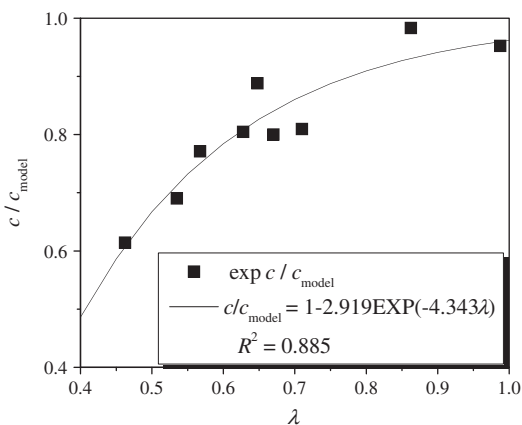


Fig. 7. Experimental ratio of c/c_{model} , obtained from the fits, versus λ . Estimates of c/c_{model} were fitted to the two parameter model $c/c_{\text{model}} = 1 - A \text{EXP}(-B\lambda)$.

solute. Coefficients c of different solutes are approaching the model value of 0.42 with the decrease of solute flux of the particular solute (Fig. 5B). Fitting the data on coefficient c to the two parameter model $c/c_{\text{model}} = 1 - A \text{EXP}(-B\lambda)$ provided a correction relation (Fig. 7) which is probably valid only for this specific membrane in this specific rectangular cell at permeation velocity of $J_v \approx 40 \mu\text{m s}^{-1}$. The proposed model of c suggests that at higher λ , already at $\lambda > 2$, c does not need correction anymore.

Correction on Sc was proposed decades ago by Gekas and Hallström [24] when significant change of diffusivity and viscosity occurs near the membrane surface under concentration polarization conditions. For instance, concentration polarization may significantly increase the viscosity of solution and decrease diffusivity of solutes near the membrane wall, which could be particularly important in ultrafiltration where permeation velocities are much higher and mass transfer coefficients much lower [36]. Concentrations used in this study, however, are too small (0.0005 – 0.02 mol dm^{-3}) to significantly affect both viscosity of solution and diffusivity of solutes near the membrane surface, even if polarization increases concentration by an order of ten. If it is assumed viscosity of solution under polarization conditions was fairly constant, which is quite reasonable, it could be that the use of theoretical (predicted) diffusivity in Sc number causes the observed differences between model and experimental data (Fig. 6). Let us assume that the value of the back-diffusion coefficient at the membrane surface is set by two opposite drags and friction forces, which is well illustrated in Fig. 3. Then the “real” back-diffusion coefficient near the membrane surface should be lower in

proportionality to solute flux through the membrane. Since mass transfer coefficient is the ratio, $k = D/\delta$, where D here is the back-diffusion coefficient, one could expect a significantly overestimated k for smaller solutes, which is clearly shown in Fig. 5A.

5. Conclusion

The difference between this and previous studies on mass transfer phenomena is in the way of varying the Sc numbers. Previous studies varied Sc numbers by using one solute (salt, dextran, glucose, etc.) and changing the viscosity, either by change in concentration of solutes, i.e. density of the solution, or simply by changing the temperature, or both. This particular study, however, varied the Sc numbers by taking the solutes that have a different diffusivity, i.e., size, in water at constant temperature and concentration, and in this context evaluated the model Sh relation from a different angle.

This study found that model Sh relation cannot be used to successfully predict mass transfer coefficient and thus concentration polarization of smaller organic solutes in SEPA II rectangular channel with one permeable wall represented by a nanofiltration membrane of defined pore size and porosity. Mass transfer coefficients of smaller organic solutes and at higher permeation velocity were significantly overestimated using model Sh relation. This was attributed to the significant solute flux of smaller solutes over the NF270 selective layer. At higher λ , $\lambda > 0.86$, when solute flux was equal or below $2.5 \mu\text{mol m}^{-2} \text{s}^{-1}$, model Sh relation was fairly valid and it predicted the mass transfer coefficients relatively well. In general, the removal of small organic solutes was found to be highly affected by the cross-flow velocity in the channel. It has been shown that increase in cross-flow velocity may increase the removal of organics from 280% to 6%, depending on the solute size.

Sc number in Sh relation needs a “solute flux” correction when significant solute flux through the NF permeable wall occurs. The present study propose such correction over a strong correlation obtained between coefficient c in, $Sh = 0.126 * Re^{0.57} Sc^c$, and λ (solute size/pore size), which is an appropriate measure of solute flux. The correlation, which has the form of $c/c_{\text{model}} = 1 - 2.919 \text{EXP}(-4.343\lambda)$, may serve to estimate coefficient c and thus correctly estimate mass transfer coefficients of differently sized organic solutes on NF270 membrane in SEPA II rectangular cell at the permeation velocity of $40 \mu\text{m s}^{-1}$.

Acknowledgements

The authors are grateful to Mr. Ivan Periša who did the major part of the experimental work in this study. This work was

supported by the Croatian Ministry of Science, Education and Sports through Project 125-1253008-3009 “*Membrane and adsorption processes for removal of organic compounds in water treatment.*”

References

- [1] B. Cyna, G. Chagneau, G. Bablon, N. Tanghe, Two years of nanofiltration at the Méry-sur-Oise plant, France, *Desalination* 147 (2002) 69–75.
- [2] Y. Bennani, K. Krešimir, E. Dražević, M. Rožić, Wastewater from wood and pulp industry treated by combination of coagulation, adsorption on modified clinoptilolite tuff and membrane processes, *Environ. Technol.* 33 (2012) 1159–1166.
- [3] S. Lee, C.-H. Lee, Effect of operating conditions on CaSO₄ scale formation mechanism in nanofiltration for water softening, *Water Res.* 34 (2000) 3854.
- [4] W. Koschuh, V.H. Thang, S. Krasteva, S. Novalin, K.D. Kulbe, Flux and retention behaviour of nanofiltration and fine ultrafiltration membranes in filtrating juice from a green biorefinery: a membrane screening, *J. Membr. Sci.* 261 (2005) 121–128.
- [5] M. Soltanieh, W. Gill, Review of reverse osmosis membranes and transport models, *Chem. Eng. Commun.* 12 (1981) 279–363.
- [6] S. Deon, P. Dutournie, P. Fievet, L. Limousy, P. Bourseau, Concentration polarization phenomenon during the nanofiltration of multi-ionic solutions: influence of the filtrated solution and operating conditions, *Water Res.* 47 (2013) 2260–2272.
- [7] A. Bouchoux, F. Lutin, Nanofiltration of glucose and sodium lactate solutions variations of retention between single- and mixed-solute solutions, *J. Membr. Sci.* 258 (2005) 123–132.
- [8] G.B.v.d. Berg, I.G. Racz, C.A. Smolders, Mass transfer coefficients in cross-flow ultrafiltration, *J. Membr. Sci.* 47 (1989).
- [9] S.S. Sablani, M.F.A. Goosen, R. Al-Belushi, M. Wilf, Concentration polarization in ultrafiltration and reverse osmosis: a critical review, *Desalination* 141 (2001) 269–289.
- [10] V. Geraldes, M.D. Afonso, Prediction of the concentration polarization in the nanofiltration/reverse osmosis of dilute multi-ionic solutions, *J. Membr. Sci.* 300 (2007) 20–27.
- [11] C. Bellona, J.E. Drewes, P. Xu, G. Amy, Factors affecting the rejection of organic solutes during NF/RO treatment—a literature review, *Water Res.* 38 (2004) 2795–2809.
- [12] P.L.T. Brian, in: U. Merten (Ed.), *Desalination by Reverse Osmosis*, M.I.T. Press, Cambridge, 1966 (Chapter 5).
- [13] C.E. Boesen, G. Jonsson, Concentration polarization in a reverse osmosis test cell, *Desalination* 21 (1977) 1–10.
- [14] C.P. Koutsou, S.G. Yiantsios, A.J. Karabelas, A numerical and experimental study of mass transfer in spacer-filled channels: effects of spacer geometrical characteristics and Schmidt number, *J. Membr. Sci.* 326 (2009) 234–251.
- [15] L. Song, Concentration polarization in a narrow reverse osmosis membrane channel, *AIChE J.* 56 (2009) 143.
- [16] A.R.D. Costa, A.G. Fane, D.E. Wiley, Spacer characterization and pressure drop modelling in spacer-filled channels for ultrafiltration, *J. Membr. Sci.* 87 (1994) 79–98.
- [17] V. Geraldes, M.D. Afonso, Generalized mass-transfer correction factor for nanofiltration and reverse osmosis, *AIChE J.* 52 (2006) 3353–3362.
- [18] V. Freger, Swelling and morphology of the skin layer of polyamide composite membranes, *Environ. Sci. Technol.* 38 (2004) 3168.
- [19] O. Coronell, B.J. Mariñas, D.G. Cahill, Depth heterogeneity of fully aromatic polyamide active layers in reverse osmosis and nanofiltration membranes, *Environ. Sci. Technol.* 45 (2011) 4513–4520.
- [20] K. Košutić, L. Kaštelan-Kunst, B. Kunst, Porosity of some commercial reverse osmosis and nanofiltration polyamide thinfilm composite membranes, *J. Membr. Sci.* 168 (2000) 101–108.
- [21] S.H. Kim, S.-Y. Kwak, T. Suzuki, Positron annihilation spectroscopic evidence to demonstrate the flux-enhancement mechanism in morphology-controlled thin-film-composite (TFC) membrane, *Environ. Sci. Technol.* 39 (2005) 1764–1770.
- [22] E. Dražević, K. Košutić, V. Dananić, D.M. Pavlović, Coating layer effect on performance of thin film nanofiltration membrane in removal of organic solutes, *Sep. Purif. Technol.* 118 (2013) 530–539.
- [23] V. Geraldes, V. Semião, M.N.d. Pinho, Flow and mass transfer modelling of nanofiltration, *J. Membr. Sci.* 191 (2001) 109–128.
- [24] V. Gekas, B. Hallström, Mass transfer in the membrane concentration polarization layer under turbulent cross flow I. Critical literature review and adaptation of existing Sherwood correlations to membrane operations, *J. Membr. Sci.* 30 (1987) 153.
- [25] G. Shock, A. Miquel, Mass transfer and pressure loss in spiral wound modules, *Desalination* 64 (1987) 339.
- [26] S. Sourirajan, T. Matsuura, in: *Reverse osmosis/ultrafiltration process principles*, National Research Council Canada, Canada, 1987, pp. 279–358 (Chapter 4).
- [27] C.R. Wilke, P. Chang, Correlation of diffusion coefficients in dilute solutions, *AIChE J.* 1 (1955) 264–270.
- [28] B.E. Poling, J.M. Prausnitz, J.P. O’Connell, *The Properties of Gases and Fluids*, McGraw-Hill, New York City, USA, 2001.
- [29] A.J.C. Semião, M. Foucher, A.I. Schäfer, Removal of adsorbing estrogenic micropollutants by nanofiltration membranes: Part B—model development, *J. Membr. Sci.* 431 (2013) 257–266.
- [30] C.A. Pacheco, I. Pinnau, M. Reinhard, J.O. Leckie, Characterization of isolated polyamide thin films of RO and NF membranes using novel TEM techniques, *J. Membr. Sci.* 358 (2010) 51–59.
- [31] C. Bellona, J.E. Drewes, P. Xu, G. Amy, Factors affecting the rejection of organic solutes during NF/RO treatment—a literature review, *Water Res.* 38 (2004) 2795–2809.
- [32] J.W. Deen, Hindered transport of large molecules in liquid-filled pores, *AIChE J.* 33 (1987) 1409–1425.
- [33] A. Ben-David, S. Bason, J. Jopp, Y. Oren, V. Freger, Partitioning of organic solutes between water and polyamide layer of RO and NF membranes: correlation to rejection, *J. Membr. Sci.* 281 (2006) 480–490.
- [34] E. Dražević, S. Bason, K. Košutić, V. Freger, Enhanced partitioning and transport of phenolic micropollutants within polyamide composite membranes, *Environ. Sci. Technol.* 46 (2012) 3377–3383.
- [35] A.R.D. Verliefde, E.R. Cornelissen, S.G.J. Heiman, E.M.V. Hoek, G.L. Amy, B.V.D. Bruggen, J.C.V. Dijk, Influence of solute-membrane affinity on rejection of uncharged organic solutes by nanofiltration membranes, *Environ. Sci. Technol.* 43 (2009) 2400–2406.
- [36] J. Schwinge, D.E. Wiley, A.G. Fane, R. Guenther, Characterization of a zigzag spacer for ultrafiltration, *J. Membr. Sci.* 172 (2000) 19.